Manganese-enhanced MRI for early detection of breast cancer metastatic potential

Joris Tchouala Nofiele[1,2], Gregory J Czarnota[2,3], and Hai-Ling Margaret Cheng[1,2]

[1]*The Hospital for Sick Children, Toronto, Ontario, Canada,* [2]*Medical Biophysics, University of Toronto, Toronto, Ontario, Canada,* [3]*Sunnybrook Health Sciences Centre, Toronto, Ontario, Canada*

TARGET AUDIENCE: Oncologist, surgeon, radiation oncologist, radiologist

PURPOSE: Highly aggressive cancer cells have a greater potential to spread (metastasize). When cancer cells escape and form tumors in distant sites, a cure is rarely possible. Unfortunately, metastasis often proceeds unnoticed until a secondary tumor has formed. One reason is that current imaging diagnosis can assess only gross physical changes, not the earliest changes at the cell level that drive cancer progression. Another reason is that invasive tissue biopsy, used to profile metastatic signatures, can sample only abnormal regions highlighted on imaging. Our aim is to augment the capability of MRI for non-invasive detection of breast cancer cell metastatic potential. This new method relies on imaging manganese (Mn) intake, a natural metal for our body, to detect aggressive cancer cells at their earliest and most curable stages. The hypothesis is that Mn can be used as a calcium analogue to probe altered calcium regulation known to be involved in cancer progression [1]. This new MRI capability brings a critically needed unique dimension to cancer imaging. It enables us to gauge the aggressiveness of cancer cells in order to characterize and appropriately treat the cancer at its earliest and most curable stages.

METHODS: Four breast cancer cell lines ranging from very metastatic to less metastatic were studied: LM2 (MDA-MB-231 selected from lung metastases [2]), MDA-MB-231, MCF7, and ZR-75-1. Cells were grown to 80-90% confluency and treated with manganese chloride ($MnCl_2$) at 0, 0.05, 0.1, 0.2, 0.5 and 1 mM for 1 hour. Cell pellets were prepared in glass vials and imaged on a 3.0 T Philips scanner (Achieva TX) using a 32-channel head coil. T1 mapping was performed using inversion recovery turbo spin echo: TR = 3000 ms, TE = 18.5 ms, 6 cm field-of-view, 3 mm slices, 0.5 x 0.5 mm in-plane resolution, and TI = [50, 100, 250, 500, 750, 1000, 1250, 1500, 2000 and 2500] ms. To assess retention of $MnCl_2$, cells were treated for 1 hour with 1mM $MnCl_2$ and then washed and given fresh medium and imaged 1 and 3 days later. Cellular uptake of manganese was quantified by preparing cells (treated and dissolved in 1M nitric acid for 30 min at 70°C) and measuring Mn2+ content with ICP-AES on a PerkinElmer spectrometer. Detection limit was 0.01 µg/mL.

RESULTS: Fig 1 shows changes in R1 (1/T1) due to $MnCl_2$ uptake in all breast cancer cell lines. Fig 2 shows the retention of $MnCl_2$ by monitoring the evolution of R1 over 3 days post-labeling. Table 1 shows ICP-AES measurements of Mn2+ content in cells.

DISCUSSION: Metastatic breast cancers (LM2, MDA-MB-231) take up significantly more $MnCl_2$ than less aggressive ones. This is supported on MRI, where R1 increases are much higher. ICP-AES supports this observation, with MDA-MB-231 showing the highest accumulation of Mn2+. Retention of $MnCl_2$ is observed only in the least aggressive cell line ZR-75-1.

CONCLUSION: This research will create a critically needed new imaging capability and offer early cellular detection of aggressive breast cancers before metastasis has occurred. Patient management and survival may be greatly improved. The concept presented can provide the basis for investigating many other solid tumors.

REFERENCES: 1. Roderick HL, Cook SJ. Nat Rev Cancer 2008; 8:361-75. 2. Munoz R et al. Cancer Res 2006; 66: 3386-91.

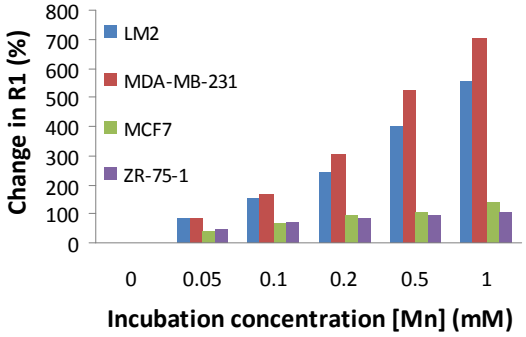

Fig 1. $MnCl_2$ uptake: changes in R1 over baseline.

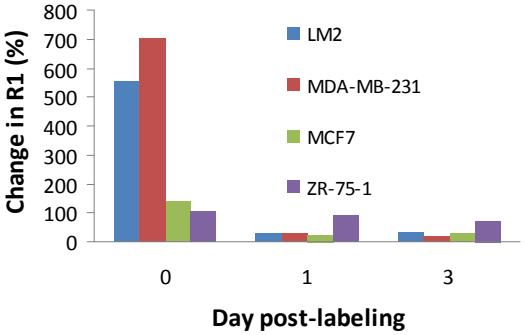

Fig 2. $MnCl_2$ retention: evolution of R1 changes over 3 days post-labeling.

Table 1. ICP-AES measurements: relative increase in Mn2+ content per cell.

[Mn2+] (mM)	LM2	MDA-MB-231	MCF7	ZR-75-1
0	1	1	1	1
0.05	4	49	10	7
0.1	11	92	8	7
0.2	17	122	19	12
0.5	27	147	17	11
1.0	32	213	29	15